

This is the accepted version of the following article:

Hassan A.H.A., Bergua J.F., Morales-Narváez E., Mekoçi A..
Validity of a single antibody-based lateral flow immunoassay
depending on graphene oxide for highly sensitive
determination of E. coli O157:H7 in minced beef and river
water. Food Chemistry, (2019). 297. 124965: - .
10.1016/j.foodchem.2019.124965,

which has been published in final form at
<https://dx.doi.org/10.1016/j.foodchem.2019.124965> ©
<https://dx.doi.org/10.1016/j.foodchem.2019.124965>. This
manuscript version is made available under the CC-BY-NC-ND
4.0 license
<http://creativecommons.org/licenses/by-nc-nd/4.0/>

1 **Validity of a single antibody-based lateral flow immunoassay depending on graphene oxide**
2 **for highly sensitive determination of *E. coli* O157:H7 in minced beef and river water**

3 Abdelrahim Hussein Abdelazeem HASSAN^{a,b}, José Francisco BERGUA^a, Eden MORALES-
4 NARVÁEZ^c, Arben MEKOÇI^{a,d,*}

5 ^aNanobioelectronics & Biosensors Group, Catalan Institute of Nanoscience and Nanotechnology
6 (ICN2), CSIC and BIST, Campus UAB, Bellaterra, 08193 Barcelona, Spain

7 ^bDepartment of Food Hygiene and Control, Faculty of Veterinary Medicine, Beni-Suef University,
8 Beni-Suef, 62511, Egypt

9 ^cBiophotonic Nanosensors Laboratory, Centro de Investigaciones en Óptica A. C, Loma del Bosque
10 115, Lomas del Campestre León, Guanajuato, 37150, Mexico

11 ^dICREA, Institució Catalana de Recerca i Estudis Avançats, Pg. Lluís Companys 23, 08010
12 Barcelona, Spain

13 *E-mail: arben.merkoci@icn2.cat

14

15

16

17

18

19

20

21

22

23

24

25

26

27 **Abstract**

28 Considering the health risks of *E. coli* O157:H7 presence in food and water, an affordable and
29 highly sensitive detection method is crucial. Herein, we report the first use of a single antibody-
30 based fluorescent lateral flow immunoassay (FLFIA) depending on non-radiative energy transfer
31 between graphene oxide and quantum dots for determination of *E. coli* O157:H7 in beef and river
32 water. FLFIA showed a high sensitivity rate thousand-fold better than the conventional lateral flow
33 (LF). In inoculated minced beef and river water samples, the limits of detection were 178 and 133
34 CFU g⁻¹ or mL⁻¹, respectively. Besides, it presented a high selectivity in the presence of other
35 possible interfering bacteria. The single antibody approach reduced the assay cost to 60% less than
36 the conventional LF. Alongside, the results could be read by portable LF readers or smartphones.
37 These advantages offer FLFIA as a promising technology for pathogen detection in food and water.

38 **Keywords**

39 Graphene oxide, fluorescent lateral flow, *E. coli* O157:H7, food safety, minced beef, water quality

40 **Chemical compounds studied in this article**

41 Phosphate buffered saline (PubChem CID: 24978514); Tween-20 (PubChem CID: 443314);

42 Graphene Oxide (PubChem CID: 124202900); Streptavidin-conjugated CdSe/ZnS quantum dots

43 (Qdot™ 655) (PubChem CID: 121237577)

44

45

46

47

48

49

50

51

52

53 **1. Introduction**

54 Foodborne and waterborne pathogens, mostly bacteria, may get into our bodies through
55 contaminated food and water leading to several health disorders varying from mild diarrhoea to
56 death, and great losses in productivity as well. *E. coli* O157:H7 is the most frequently reported
57 serotype of Shiga toxins-producing *E. coli* (STEC) in foodborne-linked hospitalizations and deaths
58 in the United States (Scallan et al., 2011). Beef has been incriminated in most food infection
59 outbreaks by *E. coli* O157:H7 (CDC, 2009). However other sources such as drinking water, dairy
60 products and vegetables were previously reported as well (Olsen et al., 2002, Islam, Doyle, Phatak,
61 Millner and Jiang, 2004, Lorusso et al., 2011, Tsiraki, Yehia, Elobeid, Osaili, Sakkas and Savvaidis,
62 2018). The health problems that could be induced by *E. coli* O157:H7 infection range from mild
63 watery diarrhoea to life-threatening conditions such as haemolytic uremic syndrome and
64 haemorrhagic colitis especially in children and the elderly (Jay, 2000). Considering the health risks
65 of *E. coli* O157:H7 and its impact on food safety, rapid, affordable and highly sensitive methods of
66 detection are necessary to monitor food and water contamination to protect the consumers from the
67 danger of that foodborne hazard.

68 The currently available methods of *E. coli* O157:H7 detection that depend on culturing and then
69 biochemical and serological examination usually take a couple of days to be completed, while
70 molecular biology-based techniques might be required for confirmation of the results. Nevertheless,
71 such conventional methods are reliable and quite accurate, they are not user-friendly as they require
72 well-trained technicians, and relatively sophisticated laboratory equipment, as well as their high
73 costs (Johnson, Brooke and Fritschel, 1998, Ngwa, Schop, Weir, León-Velarde and Odumeru, 2013,
74 Zhou, Zou, Li, Sun, Ren, and Li, 2018). Immunoassays became one of the most popular approaches
75 in analytical determination of countless kinds of pathogens in various samples, since they are
76 moderately sensitive and selective. Nonetheless, immunoassays such as ELISA and microarrays are
77 laboratory-based techniques that require multiple complex procedures to be done by well-trained
78 operators, as well as they detect *E. coli* O157:H7 in food at a limit of detection (LOD) ranges from

79 10^5 to 10^6 colony forming units per mL or g (CFU mL⁻¹ or g⁻¹) or even higher (Firstenberg-Eden
80 and Sullivan, 1997, Arbault, Buecher, Poumerol, and Sorin, 2000, Shen et al., 2014, Zhaohui,
81 Chunyang, Yingchun, and Yanbin, 2017, Kim, Jo, Mun, Noh, and Kim, 2018). Conversely, lateral
82 flow (LF) immunoassays are one of the most important analytical tools nowadays, since they are
83 simple, robust, portable, and rapid devices. Though, those conventional LF immunoassays -which
84 based on gold nanoparticles, latex beads, or quantum dots as labels- always need three antibodies;
85 one for capturing the bacteria (conjugate pad antibody), a second one for detecting the bacteria (test
86 line antibody), and a third one as a control line antibody, which means extra costs spent by such
87 devices (Berg et al., 2015, Zhang et al., 2015, Kim et al., 2018). Moreover, their LOD of *E. coli*
88 O157:H7 in water and minced beef is about 10^5 CFU mL⁻¹ or g⁻¹ (Hassan, de la Escosura-Muñiz and
89 Merkoçi, 2015). However, it has been assumed that exposure to < 100 cells of *E. coli* O157:H7 is
90 enough to induce infection in humans. As the Food and Agriculture Organization of the United
91 Nations and the World Health Organization (FAO/WHO, 2018) reported numerous food poisoning
92 outbreaks by *E. coli* O157:H7 at doses as low as 5 CFU / g of food. So, they stated that the presence
93 of *E. coli* O157:H7 at or above one CFU / 25 g constitutes a risky food commodity. Accordingly,
94 the detection of this dangerous pathogen by conventional LF assays might result valueless in
95 particularly demanding contexts. Consequently, the food and environment hygienists are in need to
96 another simple, portable and rapid device that must be affordable, highly sensitive, and highly
97 specific for rapid *in-situ* determination of *E. coli* O157:H7 in complex food matrices under the field
98 conditions.

99 Our group has been studying the quenching capabilities of graphene oxide (GO) based on the
100 fluorescence resonance energy transfer (FRET), and its interaction with photoexcited quantum dots
101 (QDs) (Morales-Narváez and Merkoçi 2012, Morales-Narváez, Hassan and Merkoçi, 2013,
102 Morales-Narváez, Naghdi, Zor, and Merkoçi, 2015; Cheeveewattanagul et al., 2017, Zamora-
103 Gálvez, Morales-Narváez, Romero and Merkoçi, 2018). We had previously patented a highly
104 sensitive pathogen-detection device for the sensing of *E. coli* in a standard buffer (Morales-Narváez

105 et al., 2013, Patent: EP 13188693.9, 2015). However, using a traditional glass slide-based
106 microarray system as a biosensing platform was quite expensive and not suitable for portability.
107 Therefore, paper-based lateral-flow assay was another low-cost option in another study done by our
108 group (Morales-Narváez et al., 2015). While, that study was limited to the detection of general *E.*
109 *coli* in buffer and bottled water by using QDs/anti-*E.coli* antibody. Although, assessment of the
110 validity of this GO-based LF immunoassay for detection of pathogenic *E. coli* O157:H7 in real
111 samples of highly complex matrices such as minced beef and river water is another hot topic worthy
112 to be investigated, since those samples are the main source of human infections by that pathogen.
113 Herein, we report the first exploit of FRET-based quenching properties of GO, and their interaction
114 with QDs for development of a fluorescent lateral flow immunoassay (FLFIA) for determination of
115 the highly pathogenic *E. coli* O157:H7 in minced beef and river water. The detection part of that
116 strip has two lines; a test line (TL) which composed of CdSe@ZnS QDs/anti-*E.coli* O157:H7
117 antibody that works as a fluorescent probe and a control line (CL) that composed of only bare QDs.
118 GO is added to the LF strip as a quencher for the fluorescent QDs after adding the sample to divulge
119 the presence of bacteria. If the sample does not have *E. coli* O157:H7, the test line will be efficiently
120 quenched when adding GO by FRET, since the distance between QDs/Abs (donor) and GO
121 (acceptor) is few nanometres (Gaudreau, Tielrooij, Prawiroatmodjo, Osmond, de Abajo, and
122 Koppens, 2013, Lin et al., 2013). On the other hand, if the sample has *E. coli* O157:H7, it will be
123 selectively captured by the specific QDs/Abs probe on the test line, then after adding GO, resonance
124 energy transfer is hindered or minimally occurs since the distance between GO and QDs exceeds to
125 more than 20 nm by the bacteria interference (Gaudreau et al., 2013, Lin et al., 2013).
126 Consequently, the fluorescence of QDs on the test line is maintained, and its intensity is
127 correlational to the concentration of the *E. coli* O157:H7 in the sample. Instead, the control line QDs
128 will be always quenched by GO because this line has not any antibodies to the target pathogen. The
129 principle and reading of FLFIA is fully illustrated in Figure 1.

130 **2. Materials and methods**

131 2.1. Reagents and equipment

132 All commercial reagents were of analytical grade and they were handled according to the safety data
133 sheets provided by the suppliers. Goat polyclonal Anti-*Escherichia coli* O157:H7 antibody
134 (conjugated with biotin) (LS-C525826-100) was purchased from LifeSpan BioSciences (Seattle,
135 WA, USA), and streptavidin-conjugated CdSe/ZnS quantum dots 655 (QDs) (Cat. No. Q10121MP)
136 were obtained from Life Technologies (Carlsbad, CA, USA). Phosphate buffered saline (PBS)
137 (PubChem CID: 24978514), bovine serum albumin (BSA), and Tween-20 (PubChem CID: 443314)
138 were purchased from Sigma-Aldrich (Madrid, Spain). Graphene oxide (GO) was bought from
139 Angstrom Materials (Ohio, U.S.A.). *Escherichia coli* O157:H7 (CECT 4783, *E. coli* O157:H7) and
140 *Salmonella enterica* subsp. *enterica* serovar Typhimurium LT2 (CECT 722T, *S. Typhimurium*)
141 strains were obtained from the Colección Española de Cultivos Tipo (CECT, Valencia, Spain). TS-
142 100 Thermo-Shaker (Biosan, Riga, Latvia) was used as a stirrer for modification of QDs with
143 antibodies. Laminated cards (HF000MC100), nitrocellulose membranes (SHF1800425), and
144 cellulose fibre (CFSP001700) that were used for fabricating FLFIA strips were purchased from
145 Millipore (Billerica, MA, USA). An IsoFlow reagent dispensing system (Imagene Technology,
146 Hanover, NH, USA) was used for dispensing the TL and CL onto the nitrocellulose membrane. A
147 Dahle 533 guillotine (Dahle, Peterborough, NH, USA) was used to cut the FLFIA strips into 6 mm
148 width. JP Selecta 2000210 oven from JP selecta (Barcelona, Spain) was used to dry the strips. A
149 portable ESEQuant lateral flow reader with its software LF-Studio Version 3.3.6 from Qiagen
150 GmbH (Stockach, Germany) were used to measure the intensities of the TL and CL of FLFIA strips.
151 As well as, fluorescent images of FLFIA strips were produced using a Typhoon 9410 Variable
152 Mode Imager (GE, Freiburg, Germany). The intensities of the lines of those fluorescent images
153 were measured using ImageJ 1.46r (Wayne Rasband, National Institutes of Health, Bethesda, MD,
154 USA). PBS (10 mM, pH 7.4) with 0.5% (v/v) Tween-20 containing 1% of BSA fraction V (w/v)
155 was employed as a standard buffer for preparation of bacterial inocula. While, PBS (10 mM, pH
156 7.4) with 0.05% (v/v) Tween-20 was used as a washing buffer. All aqueous solutions were freshly

157 prepared in Milli-Q water produced using a Milli-Q system ($>18.2 \text{ M}\Omega\text{cm}^{-1}$) purchased from
158 Millipore (Billerica, MA, USA). Scanning Electron Microscopy (SEM) images were obtained by a
159 Magellan 400L High-Resolution SEM (FEI, Hillsboro, OR, USA).

160 **2.2. Preparation of minced beef extract and bacterial inocula**

161 Minced beef was purchased from a local retail market in Barcelona and analysed by the standard
162 culturing method for the presence of *E. coli* O157 (ISO 16654:2001). Only negative samples of beef
163 and water were selected to be inoculated with bacteria. Twenty-five g of *E. coli* O157-free minced
164 beef were homogenized in a sterile stomacher bag with 225 mL of sterile PBS (10 mM, pH 7.4)
165 using a stomacher (Lab Blender 400, Seward, UK) for 3 min. Then the filtrate was used as a diluent
166 for preparation of bacterial suspensions.

167 For preparation of bacterial inocula, freeze-dried cultures of *E. coli* O157:H7 and *Salmonella*
168 Typhimurium were revived in a sterile tryptone soy broth (TSB, Oxoid Ltd., UK) and incubated at
169 37 °C for about 24 h, then transferred onto sterile tryptone soy agar (TSA, Oxoid Ltd., UK) plates
170 for another 24 h at 37 °C. Stock cultures of both strains were kept on TSA slope tubes for future use.
171 Bacterial cell suspensions were prepared directly from bacterial colonies of TSA plates, during the
172 logarithmic phase, in sterile standard buffer and river water to obtain a bacterial load of 1.5×10^8
173 CFU mL⁻¹ according to McFarland standards (McFarland, 1907) using Densimat densitometer
174 (Biomerieux, Brazil). Afterwards, ten-fold decimal bacterial dilutions (10 to 10^8 CFU mL⁻¹) were
175 prepared from the original one. Finally, heat killing of the bacteria was done by putting the bacterial
176 suspension in tightly sealed tubes to be placed in a water bath at 80 °C for 15 min to stop bacterial
177 replication. Regarding minced beef, a suitable volume of heat-killed bacterial suspension in a sterile
178 standard buffer (1.5×10^8 CFU mL⁻¹) was used to prepare ten-fold decimal dilutions of *E. coli*
179 O157:H7 in minced beef homogenate (10 to 10^8 CFU g⁻¹). The prepared bacterial dilutions were
180 stored at 4 °C until being used for the assay within two weeks in case of standard buffer and river
181 water. Whereas inoculated minced beef was used without delay to avoid sample deterioration.

182 **2.3. Fabrication of FLFIA**

183 The proposed lateral flow strips were prepared as follows: (a) assembling of the nitrocellulose
184 membrane on the laminated card. (b) Dispensing the QDs/anti-*E. coli* O157:H7 as a TL and bare
185 QDs as a CL using an IsoFlow reagent dispensing system on the nitrocellulose membrane. For TL,
186 we used a conjugate composed of 4 nM streptavidin-quantum dots 655 and 300 µg/mL biotinylated
187 anti- *E. coli* O157:H7 polyclonal antibody in standard buffer. The conjugate was prepared through
188 mixing them at 650 rpm/4 °C /30 min. Whereas for CL, we used only 4 nM of streptavidin-quantum
189 dots 655. After line dispensing, the detection pad was kept overnight inside a tightly closed
190 container in the fridge at 4 °C temperature. In the second day, the nitrocellulose membrane (2.5 × 20
191 cm) was homogenously treated with 5 mL of standard buffer, then kept in the fridge for 15 min
192 before drying in the oven at 37 °C for about 3 h. (c) Some pieces of cellulose sample and absorbent
193 pads (≈20 cm each) were saturated sequentially with Milli-Q water, and standard buffer, then they
194 were kept in the oven at 37 °C for overnight until complete dryness. (d) Afterwards, assembling the
195 sample and absorbent pads on the same laminated card. (e) Ultimately, cutting the assembled card
196 using a clean guillotine into strips of 6 mm in width. The strips were kept in a tightly closed plastic
197 container with some drying pearls in the fridge until use for bacteria determination.

198 **2.4. Using FLFIA for *E. coli* O157:H7 detection in standard buffer**

199 In order to use the prepared FLFIA strips for detection and quantification of *E. coli* O157:H7 in
200 various samples, the initial photoluminescence intensities (I_1) of both TL and CL were measured
201 using a portable lateral flow reader (Figure 1C). Then 100 µL of previously prepared *E. coli*
202 O157:H7 suspension of various concentrations in standard buffer was added onto the sample pad of
203 the fabricated strip, the strips were left for about 15 min until complete flow of the sample to the
204 absorbent pad. Afterwards, 100 µL of PBS with 0.05 % tween 20 (v/v) was dispensed on the sample
205 pad as a washing buffer, to remove any kind of intervention. Then, they were left at room
206 temperature for around 10 min until complete flow of the washing buffer. Subsequently, 100 µL of
207 aqueous solution of graphene oxide (GO) 150 µg mL⁻¹ contains 0.1 % Tween-20 (v/v) was
208 dispensed on the sample pad, for revealing the presence of bacteria. A final step of dryness was

209 done before reading the final photoluminescence intensities (I_2) of both lines using the LF reader.
210 The ratio of the final intensity to the initial one (I_2/I_1) of the test line (R_{TL}) was used as an estimation
211 for the concentration of the target bacteria in the sample.

212 **2.5. Validation of FLFIA in real samples**

213 To evaluate the overall performance of the proposed assay in real samples, artificially inoculated
214 minced beef and river water with serial concentrations of *E. coli* O157:H7 ($0, 50, 10^2, 10^3, 10^4, 10^5,$
215 and 10^6) CFU g⁻¹/mL⁻¹ were used. The same abovementioned procedure used with standard buffer
216 was conducted with real samples as well. Calibration curves were created for each sample type at
217 decimal concentrations of bacteria. The linear regression and coefficient of determination (R^2) were
218 calculated for both minced beef and river water.

219 Furthermore, spike and recovery experiment was conducted to distinguish how much the complex
220 matrix of real sample could affect the performance of our FLFIA. Two concentrations of *E. coli*
221 O157:H7 (10^3 and 10^4 CFU mL⁻¹ or g⁻¹) were spiked in each of standard buffer, minced beef, and
222 river water. At least 3 replicates were used in each concentration. The average R_{TL} of spiked minced
223 beef and river water was compared to that of standard buffer at the same concentration to estimate
224 the recovery percentage according to the following equation; recovery % = R_{TL} of real sample/ R_{TL} of
225 standard buffer.

226 As well as, the specificity of FLFIA against non-specific pathogen was tested. *Salmonella enterica*
227 subsp. enterica serovar Typhimurium (*S. Typhimurium*), a Gram-negative pathogen from the same
228 *Enterobacteriaceae* family of *E. coli* O157:H7, was used to conduct the specificity test. In this
229 experiment, we evaluated the response of FLFIA to the presence of *S. Typhimurium* either alone or
230 in a mixture with *E. coli* O157:H7, as well as it was compared with blank buffer. Blank (0 CFU mL⁻¹),
231 single *S. Typhimurium* (10^4 CFU mL⁻¹), single *E. coli* O157:H7 (10^2 and 10^4 CFU mL⁻¹), and
232 two mixtures of both bacterial species (*E. coli* O157:H7 10^2 + *S. Typhimurium* 10^4 and *E. coli*
233 O157:H7 10^4 + *S. Typhimurium* 10^2 CFU mL⁻¹) were prepared in standard buffer to conduct such
234 experiment.

235 Additionally, the reproducibility of the assay was evaluated by estimating the variation coefficient
236 through calculating the relative standard deviation (RSD %) along different batches of FLFIA strips
237 used throughout the study.

238 **3. Results and discussion**

239 **3.1. Optimization of fluorescence and quenching process**

240 Since the currently available conventional LF immunoassays based on gold nanoparticles or latex
241 beads used for *E. coli* O157:H7 detection in various food and water samples are of high costs (\approx
242 0.30 USD / test strip) and low sensitivity ($\approx 10^5$ CFU mL⁻¹ or g⁻¹) (Karakus and Salih, 2013; Hassan,
243 et al. 2015; Luo et al., 2017; Han et al., 2018), the food and water monitoring may require another
244 simple, portable, affordable and highly sensitive device. Herein, we designed a novel fluorescent
245 lateral flow immunoassay based on the interaction between photoexcited molecules and quencher.
246 We exploited streptavidin functionalized CdSe@ZnS QDs, of an approximate diameter of 14±2 nm
247 and a maximum emission wavelength at ≈ 665 nm, as donors of non-radiative energy that makes
248 them a powerful fluorescence agent. As well as, we used GO sheets in the form of water-based
249 dispersion of an average lateral dimension range of 500 nm, an average thickness of approximately
250 1.1 nm and C/O ratio of about one unit (according to manufacturer`s data), as acceptors for the non-
251 radiative energy leading to highly effectual quenching of fluorescence (Morales-Narváez et al.,
252 2013). SEM images illustrated in Figures 2C and 2C₁ show GO sheets in water suspension
253 surrounding to *E. coli* O157:H7 cells. In addition, Figure 2C₂ shows bare GO suspension of the
254 same concentration. Since the distance between the QDs and GO is very crucial for non-radiative
255 energy transfer between them as Lin et al. (2013) recorded that quenching is not strongly observable
256 at distances greater than 20 nm, so here the target bacteria ($\approx 0.5 \times 2$ μ m size) acts as a spacer
257 between the donor and the acceptor hindering the photons transfer and keeping the fluorescence of
258 QDs. Figure 2D shows a SEM micrograph of QDs-Ab conjugates are capturing to bacterial cells of
259 *E coli* O157:H7.

260 To get the most suitable photoluminescence, different concentrations of QDs (1.5, 3, 4, 6, 8, 9, and
261 10 nM) were dispensed on nitrocellulose membranes and their intensities were measured by a
262 portable LF reader (data not shown). The LF reader used in this study has an excitation wavelength
263 of 365 nm, and an emission filter of about 670 nm. Hence, 4 nM was chosen as the appropriate
264 concentration that gives about 80% of the dynamic range of the reader (Figure 1C). Additionally,
265 since the concentration of the acceptor molecules should affect the rate of photons transfer from the
266 donor to the acceptor, so, different concentrations of GO suspension in Milli-Q water (60, 70, 80,
267 100, 150 and 200 $\mu\text{g mL}^{-1}$) with two concentrations of Tween-20 (0.05 and 0.1 %) were
268 investigated to optimize the most suitable quenching conditions. The presence of Tween-20 in the
269 GO suspension aids the process of GO flow through the nitrocellulose. A hundred μL of each
270 concentration was added onto a blank strip, the TL and CL intensities were measured before and
271 after addition of GO. The degree of quenching (I_2/I_1) was calculated by dividing the final intensity
272 (I_2) by the initial one (I_1). GO 150 and 200 $\mu\text{g mL}^{-1}$ with 0.1 % Tween-20 (v/v) achieved the highest
273 quenching rates ($I_2/I_1 \approx 0.3-0.4$) (Figure 3A). However, GO 150 $\mu\text{g mL}^{-1}$ with 0.1 % Tween-20 (v/v)
274 was preferred because it achieved the most reliable results afterwards, in terms of steady
275 performance and error rate. In conclusion, 4 nM QDs and GO 150 $\mu\text{g mL}^{-1}$ with Tween-20 (0.1 %
276 v/v) were the most appropriate condition for proper photoluminescence and quenching of blank
277 strips.

278 Since bacterial cells are much bigger ($\approx 0.5 \times 2.0 \mu\text{m}$, Figure 2A) than other analytes like proteins, a
279 nitrocellulose membrane with big pore size (the diameter of the largest pore in the filtration
280 direction) was essential for our proposed assay. Moreover, there is an inverse relationship between
281 the flow rate and sensitivity of the assay, that means slow flow rate should give highly sensitive
282 assays, because it allows longer time of interaction between the antibody and the target analyte,
283 while fast flow rate reduces the sensitivity. Thus, to develop a highly sensitive assay for a big
284 analyte like bacteria, Hi-Flow 180 nitrocellulose membrane (SHF1800425) of slow flow rate (≈ 180
285 seconds/4 cm) was chosen out of others to develop our assay. Figure 2B demonstrates SEM image

286 of HF 180 nitrocellulose membrane used in this study, it proves that the pore size ($\approx 8 - 20 \mu\text{m}$) is
287 big enough to allow the proper flow of bacteria. Besides, it shows the difficulty of distinguishing
288 between bacterial cells and nitrocellulose tissue by SEM. So, all SEM images of bacterial cells
289 (Figures 2A, 2C and 2D) were prepared on silicon discs not on nitrocellulose. The total cost of each
290 strip of this fluorescent lateral flow assay was previously estimated to be ≈ 0.12 USD (Zamora-
291 Gálvez et al., 2018), which is considered about 60% less than that of conventional lateral flow strip.

292 **3.2. Optimization in standard buffer**

293 To evaluate the overall performance of the proposed FLFIA, serial concentrations of *E. coli*
294 O157:H7 ($0, 10^2, 10^3, 10^4, 10^5$ and 10^6 CFU mL^{-1}) in standard buffer were investigated. A hundred
295 μL of each concentration was loaded onto the sample pad of FLFIA strips, then followed by $100 \mu\text{L}$
296 of GO $150 \mu\text{g mL}^{-1}$ with Tween 20 (0.1 % v/v). A drying step of the strips for almost an hour in an
297 oven at 35°C before reading them using a portable lateral flow reader was essential because QDs
298 have better photoluminescence capabilities in the solid phase than the liquid one (Shi et al., 2010).
299 Afterwards, the ratio of the final intensity of TL (I_2 , after addition of GO) to the initial one (I_1 ,
300 before addition of the sample) was calculated and used as an indicator to the presence or absence of
301 *E. coli* O157:H7. We refer to it in this paper as $R_{\text{TL}} = I_2/I_1$ of TL. As high R_{TL} (close to one)
302 indicates low quenching rate and high concentration of bacteria, whereas low R_{TL} (close to zero)
303 indicates high quenching rate and low concentration or absence of bacteria. On the other hand, I_2/I_1
304 of CL = R_{CL} should be unchangeable with varying bacteria concentrations, since there are not any
305 antibodies on the CL. However, CL is essential to prove the successful flow of GO along the strip.
306 The obtained results showed an elevation in R_{TL} with increasing the concentration of bacteria in the
307 standard buffer, which means that the target *E. coli* O157:H7 is captured by the specific antibody of
308 TL (anti-*E. coli* O157:H7). However, a similar phenomenon was observed in R_{CL} as well. That
309 indicates some bacterial cells halt over CL and act as a spacer between GO and QDs there, thus
310 leading to non-specific response of CL (Figure 3B). Therefore, a washing step with $100 \mu\text{L}$ of PBS
311 with 0.05 % Tween 20 (v/v) by dispensing onto the sample pad after complete flow of the bacteria-

312 containing buffer along the strip (approximately after 15 min) was suggested to remove any kind of
313 non-specific response before addition of GO.

314 Obviously, this washing step has improved greatly that issue of non-specific response of CL,
315 leading to almost constant R_{CL} with varying concentrations of *E. coli* O157:H7 in the buffer (Figure
316 3C), while R_{TL} increased progressively with increasing the concentration of bacteria (from zero to
317 10^5 CFU mL⁻¹) and in a logarithmic manner from 50 to 10^5 CFU mL⁻¹ with R^2 equals 0.9874. Then
318 this response slightly decreased in concentrations higher than 10^5 CFU mL⁻¹ (Figure 4A, 4B). This
319 decline behaviour in response could be attributed to blocking the nitrocellulose membrane by the
320 enormous number of bacteria that lead to hindering the bacterial flow. A similar phenomenon was
321 previously reported by some literatures such as Hassan et al. (2015) who reported a decline behavior
322 in commercial gold nanoparticles-based lateral flow kits for *E. coli* O157:H7.

323 To estimate the sensitivity of FLFIA for detection of *E. coli* O157:H7 in standard buffer, the mean
324 R_{TL} of blank samples plus 3 times its standard deviation (SD) was calculated and used to determine
325 the limit of detection (LOD) of the assay. Fascinatingly, the estimated LOD of FLFIA was
326 calculated to be 57 CFU mL⁻¹ of *E. coli* O157:H7 in standard buffer (Figure 4A). This achieved
327 LOD by our assay was about thousand-fold better than the conventional lateral flow assays (LOD \approx
328 10^5 CFU mL⁻¹ or g⁻¹) that depend on a sandwich-type immunoassay on the TL and a third Ab on the
329 CL (Karakus and Salih, 2013; Hassan, et al. 2015; Luo et al., 2017; Han et al., 2018). However, the
330 proposed FLFIA requires only one antibody on the TL and without any antibodies on the CL.

331 3.3. Specificity of FLFIA

332 The specificity of immunoassays is another crucial parameter of any innovative approach. The
333 obtained results summarized in Figure 4C showed that the average R_{TL} produced by *S.*
334 Typhimurium (10^4 CFU mL⁻¹) was lower than the blank's one. Equally, the mixture of *E. coli*
335 O157:H7 10^2 + *S. Typhimurium* 10^4 CFU mL⁻¹ gave a response similar to *E. coli* O157:H7 10^2 CFU
336 mL⁻¹. Likewise, *E. coli* O157:H7 10^4 + *S. Typhimurium* 10^2 CFU mL⁻¹ and *E. coli* O157:H7 10^4
337 CFU mL⁻¹. That experiment proved the high selectivity of the proposed FLFIA to the target

338 pathogen (*E. coli* O157:H7), without any interferences from non-specific bacteria present in the
339 same medium.

340 **3.4. Using FLFIA for determination of *E. coli* O157:H7 in real samples**

341 Even though, investigation of the performance in standard buffer is quite important for the
342 optimization process, the evaluation in complex matrices is vital for validation of new methods. The
343 data illustrated in Figure 5 summarize the performance in real samples. The obtained results in
344 minced beef and river water showed a similar scenario to that of standard buffer. As R_{TL} elevated
345 regularly in a logarithmic response in concentrations from 50 to 10^5 CFU g^{-1}/mL^{-1} , with R^2 equals
346 0.9592 and 0.9542 in minced beef and river water samples, respectively. Then the response slightly
347 declined in concentrations higher than 10^5 CFU g^{-1}/mL^{-1} in both sample types, however, it is still
348 within the positive range. The same decline behaviour in response to high concentrations happened
349 with standard buffer, which confirms that this behaviour is due to the blockage of flow by the vast
350 bacterial number in higher concentrations.

351 LOD of FLFIA in minced beef and river water was estimated by calculating the averages R_{TL} of
352 FLFIA strips tested with at least 3 replicates of blank minced beef and blank river water plus 3
353 times their SD. The obtained LOD in minced beef samples was *ca.* 178 CFU g^{-1} , while it was
354 *ca.* 133 CFU mL^{-1} in river water ones (Figure 5A). The reduced sensitivity in minced beef and river
355 water than standard buffer is attributed to the matrix effect of real samples. Similar effect of the
356 sample matrix on immunoassays were previously reported by Aydin, Herzig, Jeong, Dunigan, Shah,
357 Ahn (2014), Hassan et al. (2015), Luo et al., (2017), Han et al. (2018) and Kim et al. (2018).

358 However, our achieved LODs in real samples do not affect the reliability of FLFIA and confirm its
359 high sensitivity in comparing with conventional immunoassays. The ability to detect *E. coli*
360 O157:H7 at such low concentrations without broth enrichment designates that FLFIA could be used
361 to determine as low as one CFU g^{-1} or mL^{-1} of *E. coli* O157:H7 in minced beef and water samples
362 after about 3 h of broth enrichment of the sample, since *E. coli* O157: H7 could duplicate by mitotic
363 division every 15-20 min under favourable conditions (Buchanan and Klawitter, 1993).

364 By comparing FLFIA in terms of LOD with other reported rapid methods, which were depending
365 on sandwich antibody formats, more complicated techniques and/or more expensive approaches for
366 determination of *E. coli* O157:H7 in various food samples, we noticed the high sensitivity of our
367 costless approach over those more complicated and expensive technologies. For instance, Aydin et
368 al. (2014) reported 250 CFU g⁻¹ as a LOD of *E. coli* O157:H7 in ground beef using magnetic bead-
369 based immunoassay coupled with tyramide signal amplification after 3 h of enrichment. Hassan et
370 al. (2015) reported *E. coli* O157:H7 LODs of 457 and 309 CFU g⁻¹ or mL⁻¹ in minced beef and tap
371 water samples, respectively, through using gold nanoparticles-labelled antibody sandwich-based
372 electrochemical detection. Additionally, Song, Li, Liu, Liu (2016) reported an *E. coli* O157:H7
373 LOD of 10⁵ CFU g⁻¹ or mL⁻¹ in bread, milk and jelly samples using Fluorescein isothiocyanate-
374 based immunosensor. As well as, Luo et al. (2017) compared different immunochromatographic
375 labels for lateral flow assays for *E. coli* O157:H7 determination in milk. In that study, they reported
376 LODs accounted for 1 × 10⁵, 2.5 × 10⁴, 1 × 10³, 5 × 10² CFU mL⁻¹ using gold nanoparticles,
377 quantum dots, fluorescent nanoparticles, and europium chelate nanoparticles as labels, respectively.
378 Eventually, Han et al. (2018) mentioned that the sensitivity of the nanozyme-based LFA depending
379 on a sandwich antibody format developed by them for *E. coli* O157:H7 was 900 CFU mL⁻¹ in milk.

380 **3.5. Spike and recovery test in real samples**

381 The results of spike and recovery experiment are summarized in Table (1). The recovery
382 percentages from minced beef ranged from 92.86 to 95.02 %, while those of river water ranged
383 from 95.11 to 97.98 %. Obviously, the extreme complex matrix of beef affects the assay
384 performance more than that of river water. However, it still performs in an admirable way, adequate
385 for real application requirements. Accordingly, these recovery rates demonstrate that this novel
386 approach is a promising device for determination of *E. coli* O157:H7 in food and water without any
387 interferences from the complex food and water matrices nor other competing microorganisms.

388 **3.6. Reproducibility**

389 Another important parameter for evaluating new analytical technologies is the reproducibility. In
390 this study, for executing all experiments mentioned above, we used different fabrication batches of
391 FLFIA. Among the working range of bacterial concentrations, the FLFIA strips exhibited variation
392 coefficients below 16 % in minced beef and river water. This meets the validation criterion of
393 reproducibility of new immunoassays that was stated by Findlay et al. (2000), who recommended a
394 RSD below 20 % for acceptance of new procedure in terms of reproducibility.

395 **3.7. Possibility of smartphone integration**

396 To prove the possibility of integration of proposed FLFIA into smartphones without the need to a
397 portable lateral flow reader, another device for reading the line intensities was tried. A fluorescence
398 image Typhoon scanner was used to take pictures of the strips. Then those scanned pictures were
399 analysed using ImageJ 1.46r software to determine line intensities (Figure 1B). A similar procedure
400 with smartphones could be used through a 3D-printed cassette containing an excitation LED for
401 holding the FLIFA strip to enable smartphone camera to capture the fluorescence and then an
402 ImageJ application (smartphone version) be used for analyzing the picture. This proof of concept
403 makes it a highly promising device for automation, portability, and field applications without the
404 need for a highly equipped laboratory.

405 **3.8. FLFIA versus traditional methods for detecting *E. coli* O157 in random food samples**

406 Herein, we summarize the whole procedure of using FLFIA to analyze a random unknown food
407 sample for the presence of *E. coli* O157:H7, in comparing with the traditional method in terms of
408 procedure and assay time. In case of FLFIA, firstly, 25 g or mL of the food sample is homogenized
409 or mixed with 225 mL of a pre-warmed modified tryptone soya broth plus novobiocin (mTSB+N) at
410 $41.5\text{ }^{\circ}\text{C} \pm 1\text{ }^{\circ}\text{C}$ and then incubated for 3 h. Meanwhile, the TL initial intensity of FLFIA strip being
411 recorded using a portable LF reader. Then a 100 μL of the incubated sample broth is added onto the
412 sample pad. Wait for 10 minutes to allow sample flow. Subsequently, a 100 μL of washing buffer,
413 followed by a 100 μL of GO solution are added. After strip dryness, record the TL final intensity. If
414 the R_{TL} is < 0.4 indicates a negative sample, while if it is ≥ 0.4 indicates a positive sample. Though,

415 CL should be quenched in both positive and negative samples to confirm the successful flow of
416 solutions through the strip pads. Accordingly, the total assay time of FLFIA is only 5 h, including 3
417 h of sample enrichment.

418 On the other hand, in order to detect *E. coli* O157 in food samples, using the traditional horizontal
419 method stated by the International Organization for Standardization (ISO 16654:2001) more than 60
420 h of sample examination were required to confirm the presence of this pathogen. The detection of *E.*
421 *coli* O157 by ISO's method necessitates four successive stages: a) enrichment, b) separation and
422 concentration, c) isolation and d) confirmation. Briefly, the sample was enriched in nine times the
423 weight in mTSB+N for 6 h and subsequently for a further 12 - 18 h. Then *E. coli* O157 were
424 separated and concentrated using immunomagnetic beads coated with anti-*E. coli* O157 antibodies
425 after 6 h and again, if necessary, after a further 12 - 18 h incubation. Afterwards, *E. coli* O157
426 captured with immunomagnetic particles were subcultured onto cefixime tellurite sorbitol
427 MacConkey agar (CT-SMAC) and the agar plates were incubated at 37 °C /18 - 24 h. Subsequently,
428 typical *E. coli* O157 colonies (sorbitol negative) were streaked onto nutrient agar (NA) and
429 incubated at 37 °C /18 - 24 h. Eventually, *E. coli* O157 on NA was confirmed by indole production
430 and agglutination with *E. coli* O157 antiserum. Thus, the traditional method is laborious, time
431 consuming and of high cost, as well as, it requires well-trained operators and highly equipped
432 facilities. That confirms the advantages of FLFIA over standard traditional methods.

433 **4. Conclusions**

434 In conclusion, we exclusively developed a fluorescent lateral flow immunoassay based on quantum
435 dots as donors of non-radiative energy and graphene oxide as an acceptor for such energy. We used
436 only a single antibody on the test line to capture the target pathogen, which reduced the total assay
437 cost per strip to be 60% less than the conventional LF. This study is the first report of using that
438 principle for *E. coli* O157:H7 detection in minced beef and river water. FLFIA achieved outstanding
439 LODs of *E. coli* O157:H7 (≈ 133 and 178 CFU mL⁻¹ or g⁻¹ in river water and minced beef,
440 respectively). Theoretically, this indicates the possibility of detecting as low as one CFU mL⁻¹ or g⁻¹

441 of *E. coli* O157:H7 after about 3 h of food sample enrichment in a suitable broth. The detection of
442 *E. coli* O157:H7 by FLFIA in beef complex matrix designates the ability of their using for other
443 food commodities, as well as for other similar bacterial species with changing the antibody. A
444 portable lateral flow reader was used for reading and quantifying the results. Alongside, analysing
445 the images with ImageJ software was proved to be an alternative way for reading the results with
446 smartphones. FLFIA showed numerous advantages in comparing with the standard traditional
447 method of *E. coli* O157 detection, as well as against other previously reported rapid methods.

448 **Declaration of Competing Interest**

449 The authors declare that there is no any conflict of interest in this work.

450 **Acknowledgement**

451 A.H.A. Hassan gratefully acknowledges the financial support from the Science and Technology
452 Development Fund (STDF), Egypt (Grant 25347). E. M.-N. acknowledges the financial support
453 from CONACYT (Mexico, Grant 293523) and National System of Researchers, CONACYT
454 (Mexico, Grant 74314). ICN2 is supported by the Severo Ochoa program from Spanish MINECO
455 (Grant No. SEV-2017-0706 and MAT2017) and by CERCA Programme/ Generalitat de Catalunya.

456 **References**

- 457 Arbault, P., Buecher, V., Poumerol, S., & Sorin, M. L. (2000). Study of an ELISA method for the
458 detection of *E. coli* O157 in food. In *Progress in Biotechnology* (Vol. 17, pp. 359-368). Elsevier.
459 [https://doi.org/10.1016/S0921-0423\(00\)80093-3](https://doi.org/10.1016/S0921-0423(00)80093-3).
- 460 Aydin, M., Herzig, G. P., Jeong, K. C., Dunigan, S., Shah, P., & Ahn, S. (2014). Rapid and
461 Sensitive Detection of *Escherichia coli* O157: H7 in Milk and Ground Beef Using Magnetic Bead-
462 Based Immunoassay Coupled with Tyramide Signal Amplification. *Journal of Food*
463 *Protection*, 77(1), 100-105. <https://doi:10.4315/0362-028X.JFP-13-274>.
- 464 Berg, B., Cortazar, B., Tseng, D., Ozkan, H., Feng, S., Wei, Q., Chan, R.Y.L., Burbano, J.,
465 Farooqui, Q., Lewinski, M., & Di Carlo, D. (2015). Cellphone-based hand-held microplate reader

466 for point-of-care testing of enzyme-linked immunosorbent assays. *ACS nano*, 9, 7857-7866.
467 <https://doi:10.1021/acsnano.5b03203>.

468 Buchanan R.L., & Klawitter L.A. (1992). The Effect of Incubation Temperature, Initial pH, and
469 Sodium Chloride on the Growth Kinetics of *Escherichia coli* O157:H7: *Food Microbiology*, 9, 185-
470 196. [https://doi.org/10.1016/0740-0020\(92\)80046-7](https://doi.org/10.1016/0740-0020(92)80046-7)

471 CDC, Centers for Disease Control and Prevention (2009). Reports of *E. coli* Outbreak
472 Investigations from 2006-2009, CDC, USA. URL [https://www.cdc.gov/ecoli/2006-2009-](https://www.cdc.gov/ecoli/2006-2009-outbreaks.html)
473 [outbreaks.html](https://www.cdc.gov/ecoli/2006-2009-outbreaks.html). Accessed 03.06.2019.

474 Cheeveewattanagul, N., Morales-Narváez, E., Hassan, A.-R. H., Bergua, J. F., Surareungchai, W.,
475 Somasundrum, M., & Merkoçi, A. (2017). Straightforward Immunosensing Platform Based on
476 Graphene Oxide-Decorated Nanopaper: A Highly Sensitive and Fast Biosensing
477 Approach. *Advanced Functional Materials*, 27(38), 1702741.
478 <https://doi.org/10.1002/adfm.201702741>.

479 Findlay, J. W. A., Smith, W. C., Lee, J. W., Nordblom, G. D., Das, I., DeSilva, B. S., Khan, M. N.,
480 & Bowsher, R. R. (2000). Validation of immunoassays for bioanalysis: a pharmaceutical industry
481 perspective. *Journal of pharmaceutical and biomedical analysis*, 21(6), 1249-1273.
482 [https://doi.org/10.1016/S0731-7085\(99\)00244-7](https://doi.org/10.1016/S0731-7085(99)00244-7)

483 Food and Agriculture Organization of the United Nations/ World Health Organization (FAO/WHO,
484 2008). Shiga toxin-producing *Escherichia coli* (STEC) and food: attribution, characterization, and
485 monitoring (Report). Microbiological risk assessment series 31, Rome. Available on:
486 www.fao.org/publications. Accessed 03.06.2019.

487 Gaudreau, L., Tielrooij, K. J., Prawiroatmodjo, G. E. D. K., Osmond, J., de Abajo, F. G., &
488 Koppens, F. H. L. (2013). Universal distance-scaling of nonradiative energy transfer to
489 graphene. *Nano letters*, 13 (5), 2030-2035. <https://doi:10.1021/nl400176b>

490 Han, J., Zhang, L., Hu, L., Xing, K., Lu, X., Huang, Y., Zhang, J., Lai, W. & Chen, T., (2018).
491 Nanozyme-based lateral flow assay for the sensitive detection of *Escherichia coli* O157: H7 in
492 milk. *Journal of Dairy Science*. 101:5570-5779. [https://doi:10.3168/jds.2018-14429](https://doi.org/10.3168/jds.2018-14429)

493 Hassan, A.-R. H. A.-A., de la Escosura-Muñiz, A., & Merkoçi, A. (2015). Highly sensitive and
494 rapid determination of *Escherichia coli* O157: H7 in minced beef and water using electrocatalytic
495 gold nanoparticle tags. *Biosensors and Bioelectronics*, 67, 511-515.
496 [https://doi:10.1016/j.bios.2014.09.019](https://doi.org/10.1016/j.bios.2014.09.019)

497 Islam, M., Doyle, M. P., Phatak, S. C., Millner, P., & Jiang, X., (2004). Persistence of
498 enterohemorrhagic *Escherichia coli* O157:H7 in soil and on leaf lettuce and parsley grown in fields
499 treated with contaminated manure composts or irrigation water. *Journal of Food Protection*, 67,
500 1365-1370.

501 ISO 16654:2001. Microbiology of food and animal feeding stuffs - Horizontal method for the
502 detection of *Escherichia coli* O157. URL <https://www.iso.org/standard/29821.html>. Accessed
503 03.06.2019.

504 Jay, J. (2000). Microorganisms in foods. In *Modern Food Microbiology* (6 ed.). New York: Van
505 Nostrand Reinhold.

506 Johnson, J., Brooke, C., & Fritschel, S. (1998). Comparison of the BAX for screening/*E. coli* O157:
507 H7 method with conventional methods for detection of extremely low levels of *Escherichia coli*
508 O157: H7 in ground beef. *Applied Environmental Microbiology*, 64, 4390-4395.

509 Karakus, C., & Salih, B. A. J. (2013). Comparison of lateral flow immunoassays (LFIA) for the
510 diagnosis of *Helicobacter pylori* infection. *Journal of Immunological Methods*, 396, 8-14.
511 <https://doi.org/10.1016/j.jim.2013.08.010>.

512 Kim, S. U., Jo, E.-J., Mun, H., Noh, Y., & Kim, M.-G. (2018). Ultrasensitive Detection of
513 *Escherichia coli* O157:H7 by Immunomagnetic Separation and Selective Filtration with Nitroblue
514 Tetrazolium/5-Bromo-4-chloro-3-indolyl Phosphate Signal Amplification. *Journal of Agricultural
515 and Food Chemistry*, 66, 4941–4947. [https://doi:10.1021/acs.jafc.8b00973](https://doi.org/10.1021/acs.jafc.8b00973)

516 Lin T. N., Huang L. T., Shu G.W., Yuan C. T., Shen J. L., Lin C. A. J., Chang W. H., Chiu C. H.,
517 Lin D. W., Lin C. C., & Kuo H. C. (2013). Distance dependence of energy transfer from InGaN
518 quantum wells to graphene oxide. *Optics letters*, 38 (15), 2897-2899.
519 <https://doi.org/10.1364/OL.38.002897>

520 Lorusso, V., Dambrosio, A., Quaglia, N. C., Parisi, A., Lasalandra, G., Mula, G., Virgilio, S.,
521 Lucifora, G., Dario, M., & Normanno, G. (2011). Development of a multiplex PCR for rapid
522 detection of verocytotoxin-producing *Escherichia coli* O26 in raw milk and ground beef. *Journal of*
523 *Food Protection*, 74, 13-17. <https://doi:10.4315/0362-028X.JFP-10-201>.

524 Luo, K., Hu, L. Guo, Q. Wu, C. Wu, S. Liu, D. Xiong, Y., & Lai, W. (2017). Comparison of 4
525 label-based immunochromatographic assays for the detection of *Escherichia coli* O157: H7 in milk.
526 *Journal of Dairy Science*, 100, 5176-5187. <https://doi:10.3168/jds.2017-12554>

527 McFarland, J. (1907). Nephelometer: An Instrument for Estimating the Number of Bacteria in
528 Suspensions Used for Calculating the Opsonic Index and for Vaccines. *Journal of American*
529 *Medical Association*, 14, 1176-1178. <https://doi:10.1001/jama.1907.25320140022001f>

530 Merkoçi, A., & Morales-Narváez, E. (2015). Sensitive qualitative bioassay using graphene oxide as
531 analyte revealing agent. *European Patent No. EP13188693.9*.

532 Morales-Narváez, E. & Merkoçi, A. (2012). Graphene Oxide as an Optical Biosensing Platform.
533 *Advanced Materials*, 24, 3298-3308. <https://doi.org/10.1002/adma.201200373>

534 Morales-Narváez, E., Hassan, A. R., & Merkoçi, A. (2013). Graphene Oxide as a Pathogen-
535 Revealing Agent: Sensing with a Digital-Like Response. *Angewandte Chemie International*
536 *Edition*, 52 (51), 13779-13783. <https://doi.org/10.1002/anie.201307740>.

537 Morales-Narváez, E., Naghdi, T., Zor, E., & Merkoçi, A. (2015). Photoluminescent lateral-flow
538 immunoassay revealed by graphene oxide: highly sensitive paper-based pathogen
539 detection. *Analytical Chemistry*, 87 (16), 8573-8577. <https://doi:10.1021/acs.analchem.5b02383>

540 Ngwa, G. A., Schop, R., Weir, S., León-Velarde, C. G., & Odumeru, J. A. (2013). Detection and
541 enumeration of *E. coli* O157:H7 in water samples by culture and molecular methods. *Journal of*
542 *Microbiological Methods*, 355, 92, 164–172. <https://doi.org/10.1016/j.mimet.2012.11.018>

543 Olsen, S. J., Miller, G., Kennedy, M., Higgins, C., Walford, J., McKee, G., Fox, K., Bibb, W., &
544 Mead P. (2002). A waterborne outbreak of *Escherichia coli* O157:H7 infections and hemolytic
545 uremic syndrome: implications for rural water systems. *Emerging Infectious Diseases*, 8, 370-375.
546 <https://doi:10.3201/eid0804.000218>

547 Scallan, E., Hoekstra, R. M., Angulo, F. J., Tauxe, R. V. Widdowson, M. A., Roy, S. L., Jones, J.
548 L., & Griffin, P. M. (2011). Foodborne illness acquired in the United States - major pathogens.
549 *Emerging Infectious Diseases*, 17, 7-15. <https://doi:10.3201/eid1701.P11101>.

550 Shen, Z., Hou, N., Jin, M., Qiu, Z., Wang, J., Zhang, B., Wang, X., Wang, J., Zhou, D., & Li, J.
551 (2014). A novel enzyme-linked immunosorbent assay for detection of *Escherichia coli* O157:H7
552 using immunomagnetic and beacon gold nanoparticles. *Gut Pathogens*, 6, 14.
553 <https://doi:10.1186/1757-4749-6-14>

554 Shi, X., Meng, X., Sun, L., Liu, J., Zheng, J., Gai, H., Yang, R. & Yeung, E. S. (2010) Observing
555 photophysical properties of quantum dots in air at the single molecule level: advantages in
556 microarray applications. *Lab on a Chip*, 10, 21, 2844-2847. <https://doi:10.1039/c005258b>

557 Song, C., Li, J., Liu, J., & Liu, Q. (2016) Simple sensitive rapid detection of *Escherichia coli* O157:
558 H7 in food samples by label-free immunofluorescence strip sensor. *Talanta*, 156, 42-47.
559 <https://doi.org/10.1016/j.talanta.2016.04.054>

560 Tsiraki, M. I., Yehia, H. M., Elobeid, T., Osaili, T., Sakkas, H., & Savvaidis, I. N. (2018). Viability
561 of and *Escherichia coli* O157: H7 and *Listeria monocytogenes* in a delicatessen appetizer (yogurt-
562 based) salad as affected by citrus extract (Citrox©) and storage temperature. *Food*
563 *Microbiology*, 69, 11-17. <https://doi:10.1016/j.fm.2017.07.014>

564 Zamora-Gálvez, A., Morales-Narváez, E., Romero, J., & Merkoçi, A. (2018). Photoluminescent
565 lateral flow based on non-radiative energy transfer for protein detection in human serum, *Biosensors
566 and Bioelectronics*, 100, 208-213. <https://doi:10.1016/j.bios.2017.09.013>.

567 Zhang, L., Huang, Y., Wang, J., Rong, Y., Lai, W., Zhang, J., & Chen, T. (2015). Hierarchical
568 flowerlike gold nanoparticles labeled immunochromatography test strip for highly sensitive
569 detection of *Escherichia coli* O157: H7. *Langmuir*, 31, 5537–5544.
570 <https://doi:10.1021/acs.langmuir.5b00592>

571 Zhaohui, Q., Chunyang, L., Yingchun, Fu., & Yanbin, L. (2017). Rapid and sensitive detection of *E.*
572 *coli* O157:H7 based on antimicrobial peptide functionalized magnetic nanoparticles and urease
573 catalyzed signal amplification. *Analytical Methods*, 9, 5204–5210. <https://doi:10.1039/c7ay01643c>

574 Zhou, C., Zou, H., Li, M., Sun, C., Ren, D., & Li, Y. (2018). Fiber Optic Surface Plasmon
575 Resonance Sensor for Detection of *E. coli* O157: H7 based on Antimicrobial Peptides and AgNPs-
576 rGO. *Biosensors and Bioelectronics*, 117, 347-353. <https://doi:10.1016/j.bios.2018.06.005>

577

578

579

580

581

582

583

584

585

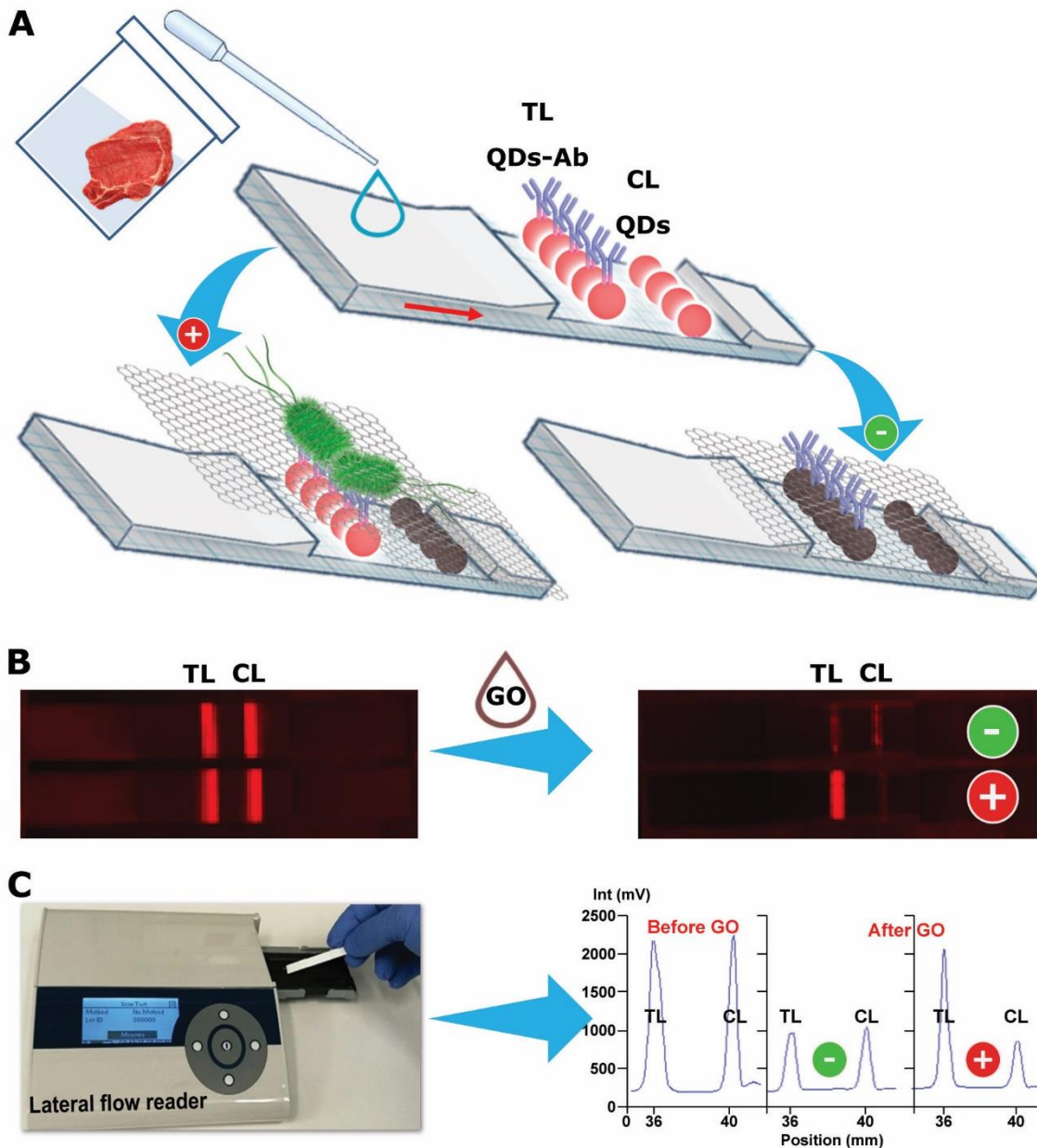
586

587

588

589

590 **Figures:**



591

592 Figure 1. Fluorescent lateral flow immunoassay (FLFIA) principle and reading. A) FLFIA strip is
593 composed of a sample pad, detection part and an absorbent pad. The detection part of FLFIA strip is
594 composed of a test line TL (Streptavidin-Quantum dots conjugated with biotinylated anti-*E. coli*
595 O157:H7 antibody “QDs-Ab”) and a control line CL (bare quantum dots “QDs”). When a beef
596 extract or water sample is added to the sample pad of FLFIA strip, it flows by capillary force
597 towards the absorbent pad. If the sample contains *E. coli* O157:H7, the bacteria will be captured by
598 specific antibody-QDs conjugate on the TL. Afterwards, graphene oxide GO is added onto the

599 sample pad. *E. coli* O157:H7 captured on the TL acts as a spacer between GO and QDs and
600 interrupts the non-radiative energy transfer between them, and this keeps the fluorescence of QDs.
601 On the other hand, the absence of the target bacteria allows the non-radiative energy transfer
602 between GO and QDs on the TL and consequently, quenches the fluorescence of QDs. B) Scanned
603 images with a fluorescence Typhoon reader of two FLFIA strips. Before addition of GO, both TL
604 and CL are fluorescing in both strips. However, after addition of GO, both TL and CL are quenched
605 in negative sample, while, TL of positive sample is still fluorescing. C) Another option of reading
606 the assay is measuring TL and CL intensities by a portable fluorescence lateral flow reader. The
607 measured fluorescence intensities (mV) of both TL and CL, before and after addition of GO to the
608 strip clarify the difference between positive (+) and negative (-) samples.

609

610

611

612

613

614

615

616

617

618

619

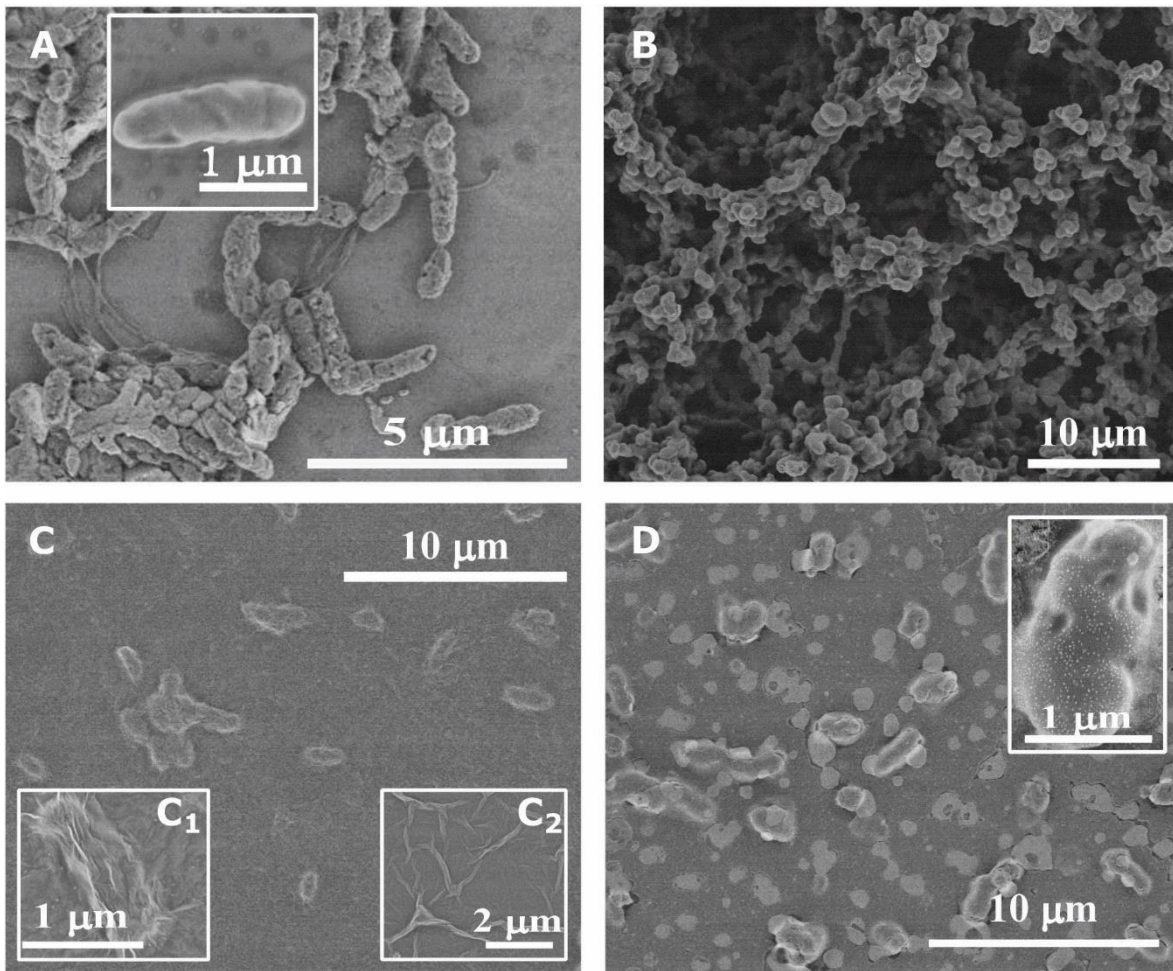
620

621

622

623

624



625

626 Figure 2. Scanning electron micrographs. A) Heat-killed *E. coli* O157:H7 (10^5 CFU mL⁻¹) in
 627 standard buffer (10 mM PBS with 0.5 % Tween-20 and 1 % BSA). B) Bare nitrocellulose
 628 membrane (Hi-Flow 180, SHF1800425) used for development of detection part of strip. C) GO
 629 sheets ($150 \mu\text{g mL}^{-1}$ with 0.1 % Tween 20) suspended in Milli-Q water, coating *E. coli* O157:H7
 630 cells. C₁) A magnified SEM image of *E. coli* O157:H7 cell is surrounded by GO sheets, C₂) Bare
 631 GO sheets. D) QDs-anti-*E. coli* O157:H7 antibody conjugates are capturing to heat-killed *E. coli*
 632 O157:H7 cells in standard buffer.

633

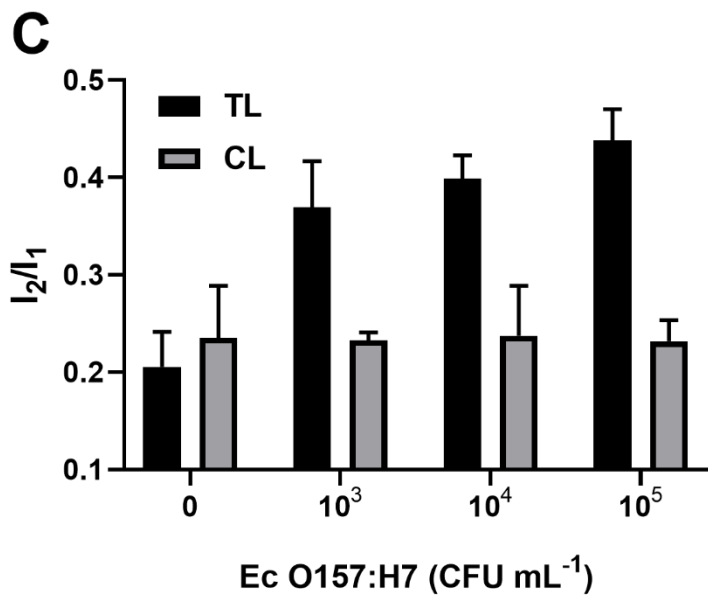
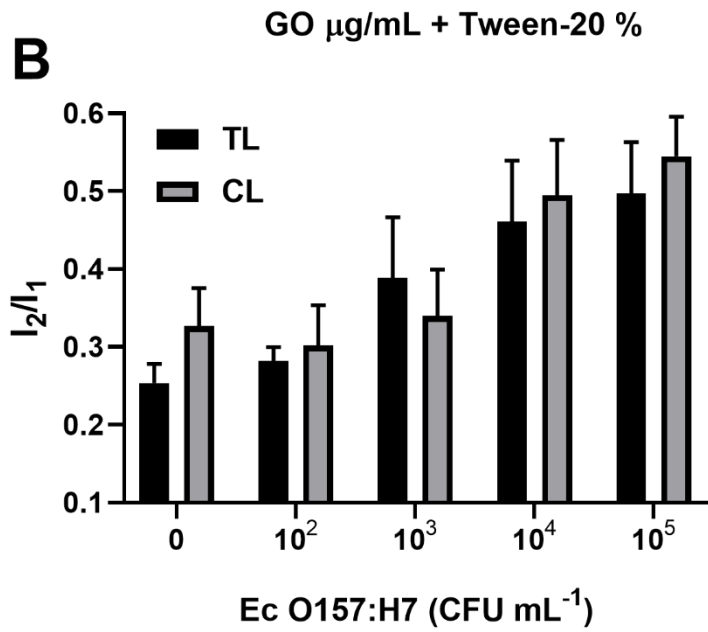
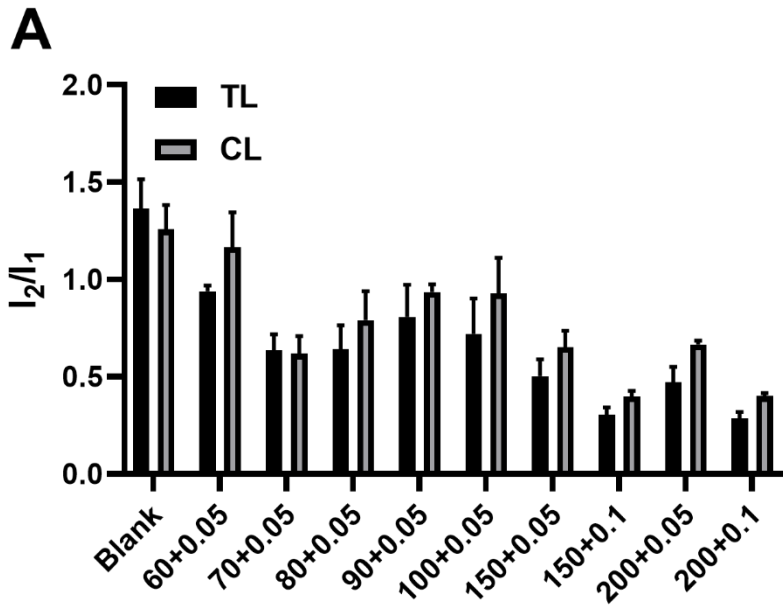
634

635

636

637

638



640 Figure 3. A) Optimization of the quenching process of QDs. Different concentrations of graphene
641 oxide (GO) suspension in Milli-Q water with Tween-20 were investigated to achieve the optimum
642 quenching conditions of both test line (TL) and control line (CL) by measuring the ratio of the final
643 intensity to the initial one (I_2/I_1) of lines. It shows that GO 150 and 200 $\mu\text{g mL}^{-1}$ with 0.1 % Tween-
644 20 are the most quenching conditions. B) and C) The significance of using a washing buffer after
645 sample loading to remove nonspecific reaction. B) Without washing step, the initial optimization
646 process exhibited a nonspecific accumulation of the bacterial cells on the CL. The I_2/I_1 of CL is
647 increasing with bacterial concentration like the TL. C) Conversely, with a washing step, nearly
648 constant I_2/I_1 of control lines were obtained regardless the bacterial concentrations in the sample.
649 The error bars represent the standard deviation of at least 3 replicates.

650

651

652

653

654

655

656

657

658

659

660

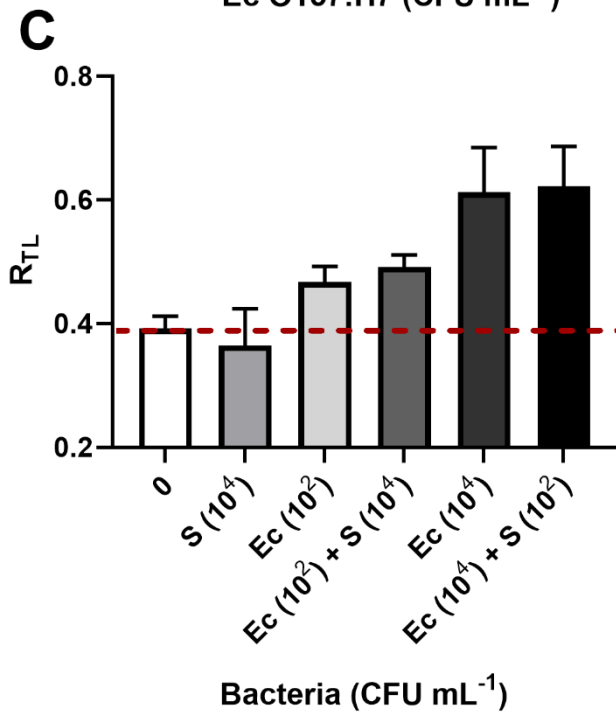
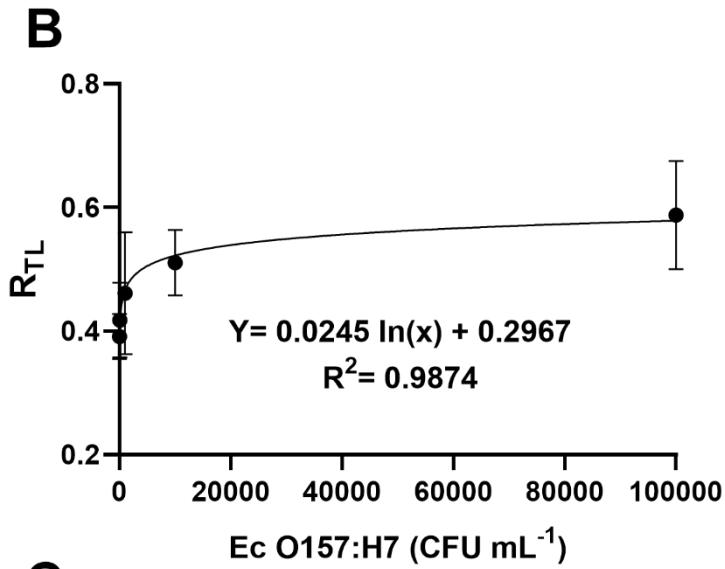
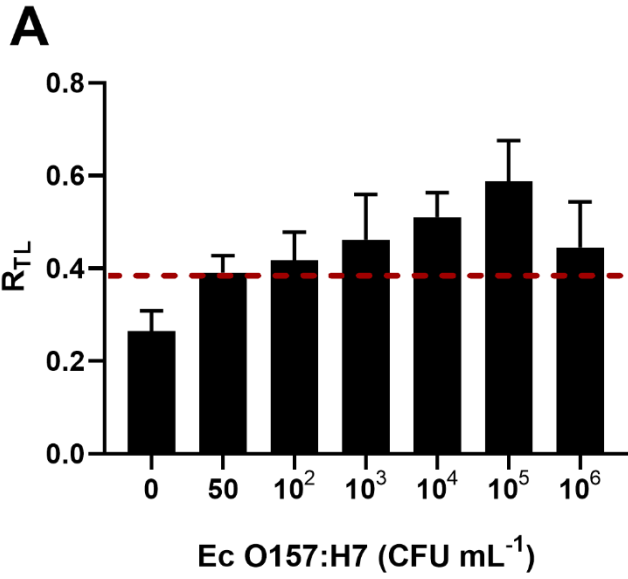
661

662

663

664

665



667 Figure 4. A) Overall response of FLFIA to various concentrations of *E. coli* O157:H7 in standard
668 buffer. Ratio of test line intensity (R_{TL})= final intensity/initial intensity of TL. B) Logarithmic
669 response of FLFIA to *E. coli* O157:H7 (Ec O157:H7) concentrations from 50 to 10^5 CFU mL⁻¹ in
670 standard buffer. C) Specificity test against higher and lower concentrations of non-specific pathogen
671 (*Salmonella* Typhimurium, S) either alone or in presence of the target pathogen, *E. coli* O157:H7
672 (Ec) were investigated. The dashed red lines (A and C) represent the limit of detection of *E. coli*
673 O157:H7 in standard buffer by FLFIA (≈ 57 CFU/ mL), which was estimated as the mean value of
674 blank buffer R_{TL} plus three times its SD. The error bars represent the standard deviation of at least 3
675 replicates.

676

677

678

679

680

681

682

683

684

685

686

687

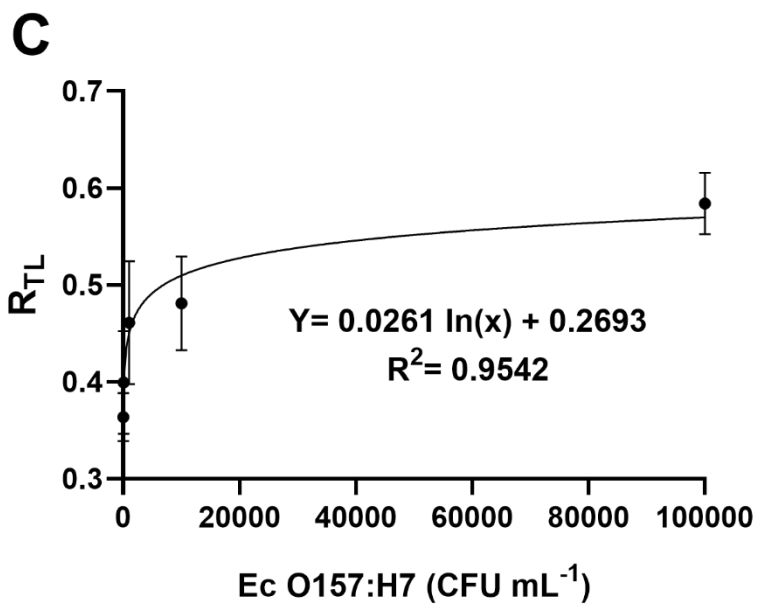
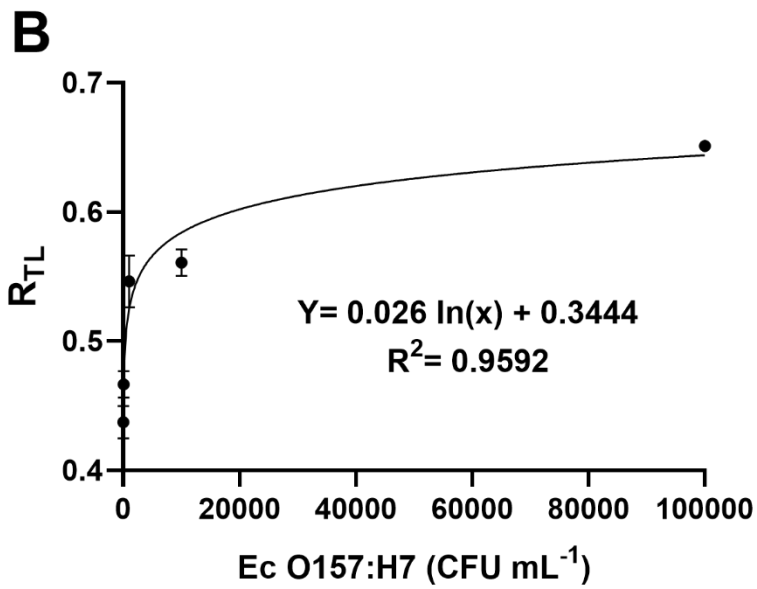
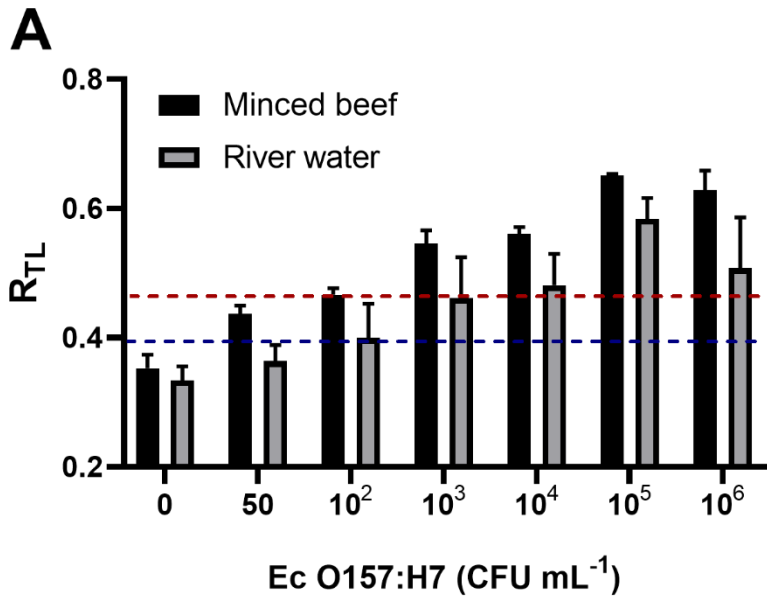
688

689

690

691

692



694 Figure 5. A) Overall response of FLFIA strips to various concentrations of *E. coli* O157:H7 (*Ec*
695 O157:H7) in minced beef and river water samples. The dashed lines represent the limit of detection
696 of *E. coli* O157:H7 in minced beef (red) and water (blue) (≈ 178 and 133 CFU g^{-1} or mL^{-1}
697 respectively), which were calculated as the R_{TL} mean value of blank minced beef or river water plus
698 three times their SD. B) Logarithmic response of FLFIA to *E. coli* O157:H7 concentrations from 50
699 to 10^5 CFU g^{-1} in minced beef. C) Logarithmic response of FLFIA to *E. coli* O157:H7
700 concentrations from 50 to 10^5 CFU g^{-1} in river water. The error bars represent the standard deviation
701 of at least 3 replicates.

702

703

704

705

706

707

708

709

710

711

712

713

714

715

716

717

718

719

720 **Tables**

721 Table 1. Spike and recovery experiment in minced beef and river water.

Real samples (n ≥ 3)	Initial level of <i>Ec</i> O157:H7 (CFU mL ⁻¹ or g ⁻¹)	Spiked value of <i>Ec</i> O157:H7 (CFU mL ⁻¹ or g ⁻¹)	R _{TL} in standard buffer	R _{TL} in real samples	Recovery (%)
River water	0.0	10 ³	0.419	0.411	97.98
	0.0	10 ⁴	0.559	0.532	95.11
Minced beef	0.0	10 ³	0.419	0.398	95.02
	0.0	10 ⁴	0.559	0.501	92.86

722 Where, n, number of replicates. R_{TL}, Ratio of test line intensity= final intensity/initial intensity of
723 test line. *Ec* O157:H7, *E. coli* O157:H7. CFU, colony forming units.

724

725